

# Restoring natural sensory feedback in real-time bidirectional hand prostheses

S. Raspopovic, M. Capogrosso, F. Petrini, M. Bonizzato, J. Rigosa, G. Di Pino, J. Carpaneto, M. Controzzi, T. Boretius, E. Fernandez, G. Granata, C. M. Oddo, L. Citi, A.L. Ciano, C. Cipriani, M.C. Carrozza, W. Jensen, E. Guglielmelli, T. Stieglitz, P.M. Rossini, S. Micera

This is the author's version of the work. It is posted here by permission of the AAAS for personal use, not for redistribution. The definitive version was published in Science Translational Medicine on Vol. 6, issue 222 5 February 2015, DOI: 10.1126/scitranslmed.3006820.

Link: <http://stm.sciencemag.org/content/6/222/222ra19>

# **Title: Restoring natural sensory feedback in real-time bidirectional hand prostheses**

**Authors:** S. Raspopovic<sup>1,2</sup>, M. Capogrosso<sup>1,2</sup>§, F. Petrini<sup>3,4</sup>§, M. Bonizzato<sup>2</sup>§, J. Rigosa<sup>1</sup>, G. Di Pino<sup>3,5</sup>, J. Carpaneto<sup>1</sup>, M. Controzzi<sup>1</sup>, T. Boretius<sup>6</sup>, E. Fernandez<sup>7</sup>, G. Granata<sup>4</sup>, C. M. Oddo<sup>1</sup>, L. Citi<sup>8</sup>, A.L. Ciano<sup>3</sup>, C. Cipriani<sup>1</sup>, M.C. Carrozza<sup>1</sup>, W. Jensen<sup>9</sup>, E. Guglielmelli<sup>3</sup>, T. Stieglitz<sup>6</sup>, P.M. Rossini<sup>4,7\*</sup>, S. Micera<sup>1,2\*</sup>

## **Affiliations:**

<sup>1</sup>The BioRobotics Institute, Scuola Superiore Sant'Anna, Pisa, Italy

<sup>2</sup>Translational Neural Engineering Laboratory, Center for Neuroprosthetics and Institute of Bioengineering, School of Engineering, Ecole Polytechnique Federale de Lausanne, Lausanne, Switzerland

<sup>3</sup>Laboratory of Biomedical Robotics & Biomicrosystems, Campus Bio-Medico University, Rome, Italy

<sup>4</sup>IRCCS San Raffaele Pisana, Rome, Italy

<sup>5</sup>Institute of Neurology, Campus Bio-Medico University, Rome, Italy

<sup>6</sup>Laboratory for Biomedical Microtechnology, Department of Microsystems Engineering – IMTEK, University of Freiburg, Freiburg, Germany

<sup>7</sup>Catholic University of The Sacred Heart, Rome, Italy

<sup>8</sup>University of Essex, United Kingdom

<sup>9</sup>Center for Sensory-Motor Interaction, Department of Health Science and Technology, Aalborg University, Aalborg, Denmark

\*Equal contribution. Correspondence to: [silvestro.micera@epfl.ch](mailto:silvestro.micera@epfl.ch) [[@sssup.it](mailto:@sssup.it)] and [paolomaria.rossini@rm.unicatt.it](mailto:paolomaria.rossini@rm.unicatt.it)

§Equal contribution

**Abstract:** The hand is a high-performance system, the amputation of which causes severe disability. The usability of current hand prostheses is limited by the poor sensory feedback available to the user while grasping. Here we show that by stimulating the sensory peripheral nerves, natural sensory information can be provided to an individual with hand amputation during the real-time control of a dexterous prosthesis. This feedback enabled the participant to effectively control the grasping force of the prosthesis, in the absence of visual and auditory feedback. In addition, by exploiting the restored sensations, the participant was able to blindly identify the compliance and shape of different objects. Our approach can significantly improve the efficacy of hand prostheses, thus enabling them to become a near natural replacement for missing hands.

**One Sentence Summary:** We developed real-time bidirectional hand prosthesis able to deliver a homologous sensory (touch/pressure) feedback to an amputee allowing for a fine force control of the hand and realistic object sensing.

**Main Text:** Dexterous hand control is a characterizing feature in the evolutionary process that has shaped the particular characteristics of higher primates (1). Hand amputation results in a highly disabling traumatic event that affects the quality of life of millions of people worldwide. Hand prostheses should be able to mimic the biomechanical structure of the natural hand and to restore the bidirectional link between the user's nervous system and the device, by exploiting the post-amputation persistence of the neural networks devoted to hand and finger motor control in the brain (2). The first modern prosthetic hand was developed at the beginning of the 20th century (3) and the first functional myoelectric prostheses were created 60 years ago (4, 5). After the concept of proportional control introduced in (6), the prosthesis-user interface has not been significantly revisited until recently. At the same time, significant advances have been carried out towards the development of dexterous and sensorized hand prostheses (7). These developments made even more compelling the need for a more effective bidirectional control. A promising solution, especially for proximal amputations (i.e., near the axilla), is provided by targeted muscle reinnervation (TMR) (8, 9). With this approach it is possible to design prostheses chronically used by individuals with arm/hand amputation that could provide certain amount of sensory feedback (10, 11), and that enable a certain degree of embodiment of the prosthesis (12). However, since the superficial electromyogram (sEMG) used as a control signal is recorded from the same area that needs to be mechanically stimulated to provide feedback, TMR subjects are unable to contract muscles and simultaneously perceive a touch sensation (13). On the other hand, the rapid development of neural interfaces for the peripheral nervous system (14) has opened up the potential for new tools through which bidirectional communication with nerves in the stump could be potentially performed. Initial feasibility demonstrations of the induction of some sensations (15) and preliminary trials of the sporadic control of non-attached prostheses (16, 17) have recently been achieved. However, until now no proof has been accumulated for the real-time use of these neural interfaces for the effective bidirectional control of multi degree-of-freedom prosthetic hands.

Reliable, real-time, and natural feedback from the hand prosthesis to the user is essential in order to enhance the control and functional impact of prosthetic hands in daily activities, therefore prompting the full acceptance by the users (18, 19). Manipulation is achieved as the result of the complex relationship between motor commands and sensory feedback during hand activities (20, 21). The restoration of the natural flow of sensory information should therefore lead to the high performance use of hand prostheses, without requiring continuous visual monitoring. Furthermore, by exploiting the preserved residual motor networks and pathways (22) to close the prosthetic control loop, a significant decrease in the associated cognitive burden compared to any non-natural approach (23) should be obtained. We propose the term “restored sensation” to represent the concept of real-time natural feedback discernible by the prosthesis user.

In this study our aim was to restore the sensation of touch in the missing hand, using intraneural electrodes that deliver electric stimuli to the peripheral sensory nerves, proportionally to hand prosthesis sensors readouts, and to verify whether the participant was able to use this sensory information during the real-time control of the prosthetic hand (Fig. 1). Critical to the accomplishment of such a task is the total time taken to integrate the sensory feedback from the onset of contact reported by the finger sensor of the prosthesis. We managed to keep the time below 100 ms (sup. mat.), which is nearly imperceptible to the user (24). Experiments were performed with participant DAS who had suffered a post-traumatic transradial left arm amputation 10 years ago. He was surgically implanted with four TIME electrodes (25) (two in the ulnar and two in the median nerves), with a total of 56 active stimulating and 8 grounding

sites, throughout the experiment. Sensations elicited by the electrical stimulation of nerves corresponded to the physiological sensory mapping of touch/pressure within the innervation territories of the median (26) and ulnar (27) nerves, showing that this ability is not lost even several years after sensory deprivation due to nerve truncation (fig. S1). After three weeks of sensory mapping, which was verified to be stable in sensation delivering, the user was equipped with the hand prosthesis (7) by means of a custom-made socket. The decoding of the user's intention to perform different grasps or to open the hand was performed using sEMG signals (fig. S2).

First we performed experiments to assess whether the natural dynamic sensory feedback could lead to the voluntary and reliable modulation of the grasping force of the hand prosthesis. During these trials, the participant was blindfolded and acoustically shielded (Fig. 1), and was asked to produce three different force levels using pinch, ulnar, or palmar grasps (fig. S2), on a pressure sensor chamber shaped like a daily life object (*a cream tube*).

The participant was able to accurately control the grasp force by index and thumb or by little finger, in both single-level press-and-release trials and in the continuously modulated so-called “staircase task”, (Fig. 2a) in which he had to gradually increase the level of force, holding the object with a stable force during the intervals separating various steps and then gradually return to the baseline. Results clearly showed that he was able to produce three levels of stable and discrete pressure with both the index and the little finger under voluntary control, with a success rate of over 90% (Fig. 2b). Remarkably, he was able to adjust his force levels whenever he realized (thanks to the restored sensation) that he had exerted too much pressure. He released the grasp back on contact and then adjusted the force to the correct level, as highlighted in Fig. 2a, in the case of the ‘low force’ trial of the little finger. In order to verify that these were clear and exclusive effects of the integration of the dynamic sensory feedback induced with nerve stimulation, during some trials he was instructed to apply a minimum level of force, while the feedback from the hand prosthesis was switched off (see placebos in fig. S3). He was unable to achieve any kind of voluntary controlled force in all these control trials.

The accuracy of execution increased from the first day until the end of the experiment, showing that the subject had undergone a clear learning process in integrating the restored sensation into the closed-loop control (Fig. 2b). In order to compare performances of the “sensorized” hand prosthesis to those of the intact hand for this specific task, the participant was asked to perform the same task with his healthy (and dominant) right hand. A comparison of the performances with the healthy hand revealed that the force profile obtained by the subject when using the hand prosthesis, with the restored sensation but with no visual and auditory feedback, was remarkably similar (Fig. 2c) to the healthy hand profile ( $R^2=0.8$ ), compared to that of the hand prosthesis without the restored tactile feedback but with the visual and acoustic cues ( $R^2=0.5$ ). Paradoxically, the latter condition corresponds to the best-performing scenario with the currently available prostheses without sensory feedback.

We also investigated whether the participant was able to integrate multiple and independent pressure sensory inputs related to index, thumb, and little fingers to control the grasping force during a palmar grasp. Results showed (Fig. 2d) that the subject managed to integrate the multisensory dynamic information, with 93% overall accuracy. Consequently, the participant mastered a fine closed-loop control, featuring an emerging higher level of complexity, thus demonstrating the rehabilitative potential of this approach in combining single sensations simultaneously dispatched along separate neural pathways in a comprehensive, physiological and functional prosthetic agency experience. In order to exclude the possibility that the participant

could have learnt to control the force by associating it with the time necessary for the hand prosthesis closure a new test was carried out where three different velocities of hand actuation were used in random order and in a completely blind condition. Results showed a nearly identical level of high performance, confirming that the control exhibited was entirely due to the induced sensory feedback (fig. S3).

After confirming that the subject managed to integrate the restored sensation by modulating the force control, we wanted to explore its possible integration in an “ecological” condition of hand use. During the manipulation task (fig. S4), the participant was instructed to recognize an object's position with respect to the hand and to perform the most appropriate grasp. Three objects were placed at different locations, close to the robotic hand: a long cylindrical object covering the whole hand and two small objects located in the radial or ulnar sides. By exploiting the induced feedback, during the explorative phase of the task, the participant had to understand where the object was placed, then to perform the location-appropriate grasp (palmar, pinch, or ulnar), and finally to displace the object by lifting and moving it. A series of three exploration trials are shown in Fig. 3a, displaying a typical sEMG envelope pattern, the predicted motor commands for the hand prosthesis, the hand sensor readings, as well as the stimulation currents inducing the restored sensation. He was able to perform the exploration task and functional grasping with an average accuracy of 97% (Fig. 3b and movie S1). These results showed that the feedback provided by intraneural stimulation is extremely useful in order to achieve the skillful control of the prosthesis in common functional tasks - even without visual or acoustic cues.

We then verified whether the participant could use the restored sensation to identify the physical properties of an object, such as compliance and shape. Even though gathering object compliance is a complex task achieved with multi-sensory integration (28), we hypothesized that the restored sensation could be exploited to discriminate between stiffer and softer objects, using the subject's cognitive ability to decode the level of stiffness by processing the artificial tactile feedback from the robotic hand sensors. The participant was thus provided with three objects with different compliances: a piece of wood (hard), a short stack of plastic glasses (medium), and a packet of cotton (soft). He was instructed to grasp the object with a palmar grasp and to apply force until he was able to understand the compliance of the object (Fig. 4a). Remarkably, after just three sessions the participant was able to identify the compliance of all three objects (Fig. 4b and movie S2).

As expected, while the subject was pinching an object, the output of the tension sensor in the hand changed with the compliance of the object being tested: the stiffer the object, the more rapidly the output of the sensor was saturated. Consequently (Fig. 4a), the intensity of the stimulation current reached the maximum more rapidly when the stiff object was pinched, than with the soft object.

The average amplitude current derivative, computed during pinch, reflected this phenomenon (Fig. 4b). The highest value (Mean  $\pm$  s.d. :  $0.61 \pm 0.26$ ) was obtained with the stiff object, while the medium value ( $0.23 \pm 0.07$ ) and the lowest value ( $0.11 \pm 0.036$ ) were reported with the medium compliance and soft objects, respectively, being statistically three-wise different ( $p < 0.001$ ). We hypothesize that the subject might have exploited the average velocity of change in the injected current delivered during the task to distinguish between three different object compliances. This would be a close-to natural (28) artificial neural code, rapidly learnt and memorized for the on-line control of the hand prosthesis.

Finally, we tested whether the participant was able to use the restored sensations on both radial and ulnar sides of the hand to recognize different object shapes. In order to do so, we presented

three items (Fig. 4c): a relatively large cylindrical object (a bottle), a medium-large spherical object (a baseball), and a small spherical object (a mandarin orange). The participant was able to correctly classify all the three shapes with an average accuracy of 88% (Fig. 4d). Interestingly, although the baseball was big enough to cover the entire hand, the subject could feel that the spherical shape produced a different sensation than the cylindrical bottle. We hypothesize that to achieve this discrimination ability the participant used the perceived delay between the index and little finger contact with the object surface provided by the neural stimulation when grasping the spherical shape. This delay was in fact statistically different between the spherical and the cylindrical shapes ( $p < 0.01$ , Fig. 4d). To confirm position independence in recognizing smaller objects, we presented them both in the ulnar and radial positions, without reducing the discrimination ability (fig. S5a-b). The subject showed the ability to understand the object shape faster already after the first trials of the same session (fig. S5c).

The participant abilities to finely control grasping force, to execute functional manipulations, together with his capacity to identify different compliances and shapes are a powerful evidence of the impact that our approach could have in real-life conditions. The use of real-time and homologues neural stimulation emulates natural sensory information transmission during hand/fingers object manipulation. With this form of feedback, the subject was able to effectively integrate sensory stimuli delivered to different nerves. In addition, this approach enhances the brain's ability to compensate for inaccuracies in the hand prosthesis in decoding motor commands as reflected by sEMG signals.

The way the user integrated the compliance information is similar to the innate sensory loop of a natural hand: upon squeezing the object with fingertips, normal contact forces arise, causing the deformation of both fingertips and objects. The parameter coded by the hand/finger receptors is the average slope of the curve force-time associated with the fingertips (28). The stiffer the object is, the higher the average slope is perceived to be, similar to what we achieved with artificial sensations. Likewise, the sensory feedback naturally received while exploring an object shape is a complex mixture of redundant and overlapping information coming from different sensory fibers. However, as shown in our case, even sensing a differential recruitment of two parts of the hand is sufficient to recognize the overall shape of some familiar objects. The restored sensation induces an artificial, although close-to-natural, neural coding and its combined use on multiple channels provides clear evidence of the build-up of sensations as a consequence of the natural and real-time properties of this neural coding.

The concept of our closed-loop bidirectional neural interface could be extended to enable stimulating a larger number of sites on the nerve implants with the readouts of as many sensors that can potentially be embedded in a robotic hand, thus delivering a wider variety of sensations to the user. This technology may offer greater advantages to subjects with bilateral amputations, who need functional replacement, since they are deprived of the ability to recognize the compliance, or shape of objects, compared to people with unilateral amputation who can do it with their healthy hand.

Finally, by exploiting our concept of restored sensing, the controllability and functionality of prostheses will very likely be enhanced, eventually reducing the cognitive burden required in using them. This should thus help to promote the acceptance of prosthetic hands, improving the overall quality of life of users.

## References and Notes:

1. A.W. Goodwin, H.E. Wheat, Sensory signals in neural populations underlying tactile perception and manipulation. *Annu Rev Neurosci.* 27, 53-77 (2004).
2. K.T. Reilly, C. Mercier, M.H. Schieber, A. Sirigu, Persistent hand motor commands in the amputees' brain. *Brain* 129, 2211–23 (2006).
3. Schlesinger, G. Der Mechanische Aufbau der Kunstlichen Glieder, pt. 2. *„Ersatzglieder und Arbeitshilfen*. Berlin: Springer, (1919).
4. R. Reiter, “Eine neu elektrokunstand,” *Grenzgebiete Med.* 1, 133–135 (1948).
5. A.Y. Kobrinski, Bioelectric control of prosthetic devices. *Herald of the Academy of Science-USSR* 30, 58-61 (1960).
6. A. Bottomley, Myoelectric Control of Powered Prostheses. *J. Bone & Joint Surg.* 47B, 411-415 (1965).
7. M. C. Carrozza, G. Cappiello, S. Micera, B. B. Edin, L. Beccai, *et al*, Design of a cybernetic hand for perception and action. *Biol. Cybern.* 95, 629–644 (2006).
8. T. A. Kuiken, L. A. Miller, R. D. Lipschutz, B. A. Lock, K. Stubblefield, *et al.*, Targeted reinnervation for enhanced prosthetic arm function in a woman with a proximal amputation: a case study. *Lancet* 369, 371–380 (2007).
9. T. A. Kuiken, G. Li, B. A. Lock, R. D. Lipschutz, L. A. Miller, *et al.*, Targeted muscle reinnervation for real-time myoelectric control of multifunction artificial arms. *JAMA* 301, , 619–628 (2009).
10. P.D. Marasco, A.E. Schultz, T.A. Kuiken, Sensory capacity of reinnervated skin after redirection of amputated upper limb nerves to the chest. *Brain* 132, 1441–8 (2009).
11. T. A. Kuiken, P.D. Marasco, B. Lock, R. Harden, and J. Dewald, Redirection of cutaneous sensation from the hand to the chest skin of human amputees with targeted reinnervation. *Proc. Natl. Acad. Sci. USA* 104, 20061–6 (2007).
12. P. D. Marasco, K. Kim, J. E. Colgate, M. A. Peshkin, and T. A. Kuiken, “Robotic touch shifts perception of embodiment to a prosthesis in targeted reinnervation amputees,” *Brain* 134, 747–758 (2011).
13. K. Kim, J.E. Colgate, Haptic feedback enhances grip force control of sEMG-controlled prosthetic hands in targeted reinnervation amputees. *IEEE Trans. Neural. Syst. Rehabil. Eng.* 20, 798-805 (2012).
14. X. Navarro, T. Krueger, N. Lago, S. Micera, T. Stieglitz, *et al*, A critical review of interfaces with the peripheral nervous system for the control of neuroprostheses and hybrid bionic systems. *J. Peripher. Nerv. System* 10, 229–258 (2005).

15. G. S. Dhillon, T. B. Kruger, J. S. Sandhu, and K. W. Horch, Effects of short-term training on sensory and motor function in severed nerves of long-term human amputees. *J Neurophysiol.* 93, 2625–2633 (2005).
16. X. Jia X, M.A. Koenig, X. Zhang, J. Zhang J, T. Chen, *et al*, Residual motor signal in longterm human severed peripheral nerves and feasibility of neural signal controlled artificial limb. *J Hand Surg. Am.* 32, 657–66 (2007).
17. P. M. Rossini, S. Micera, A. Benvenuto, J. Carpaneto, G. Cavallo, *et al.*, Double nerve intraneural interface implant on a human amputee for robotic hand control. *Clin. Neurophysiol.* 121, 777–783 (2010).
18. D. Atkins, D. Heard, W. Donovan, Epidemiologic overview of individuals with upper-limb loss and their reported research priorities. *J Prosthet. Orthot.* 8, 2–11 (1996).
19. E. Biddiss, D. Beaton, T. Chau, Consumer design priorities for upper limb prosthetics. *Disabil. Rehabil. Assist. Technol.* 2, 346–57 (2006).
20. R.S. Johansson, J.R. Flanagan, Coding and use of tactile signals from the fingertips in object manipulation tasks. *Nat. Rev. Neurosci.* 10, 345–59 (2009).
21. J.R. Flanagan, M.C. Bowman, R.S. Johansson, Control strategies in object manipulation tasks. *Curr. Opin. Neurobiol.* 16, 650–9 (2006).
22. W. Schady, S. Braune, S. Watson, H.E. Torebjörk, R. Schmidt, Responsiveness of the somatosensory system after nerve injury and amputation in the human hand. *Ann. Neurol.* 36, 68–75 (1994).
23. K.A. Kaczmarek, J. G. Webster, P. Bach-y-Rita, W.J. Tompkins, Electrotactile and vibrotactile displays for sensory substitution systems. *IEEE Trans. Biomed. Eng.* 38, 1–16 (1991).
24. T.R. Farrell, R.F. Weir, The optimal controller delay for myoelectric prostheses. *IEEE Trans. Neural. Syst. Rehabil. Eng.* 15, 111–8 (2007).
25. T. Boretius, J. Badia, A. Pascual-Font, M. Schuettler, X. Navarro, *et al.*, A transverse intrafascicular multichannel electrode (time) to interface with the peripheral nerve. *Biosens. Bio- electron.* 26, 62–69 (2010).
26. W. Schady, J. L. Ochoa, H. E. Torebjörk, and L. S. Chen, Peripheral projections of fascicles in the human median nerve. *Brain* 106, 745–760 (1983).
27. P. Marchettini, M. Cline, J.L. Ochoa, Innervation territories for touch and pain afferents of single fascicles of the human ulnar nerve. Mapping through intraneural microrecording and microstimulation. *Brain* 113, 1491–500 (1990).
28. M. A. Srinivasan and R. H. LaMotte, Tactual discrimination of softness. *J. Neurophysiol.* 73, 88–101 (1995).



Supplementary Materials

Materials and Methods

Figs. S1, S2, S3, S4, S5

References (29-30)

Movies S1, S2

**Acknowledgments.** This work was supported by the EU Grant CP-FP-INFOSO 224012 (TIME project) and by the project NEMESIS (Neurocontrolled mechatronic hand prosthesis) funded by the Italian Ministry of Health.

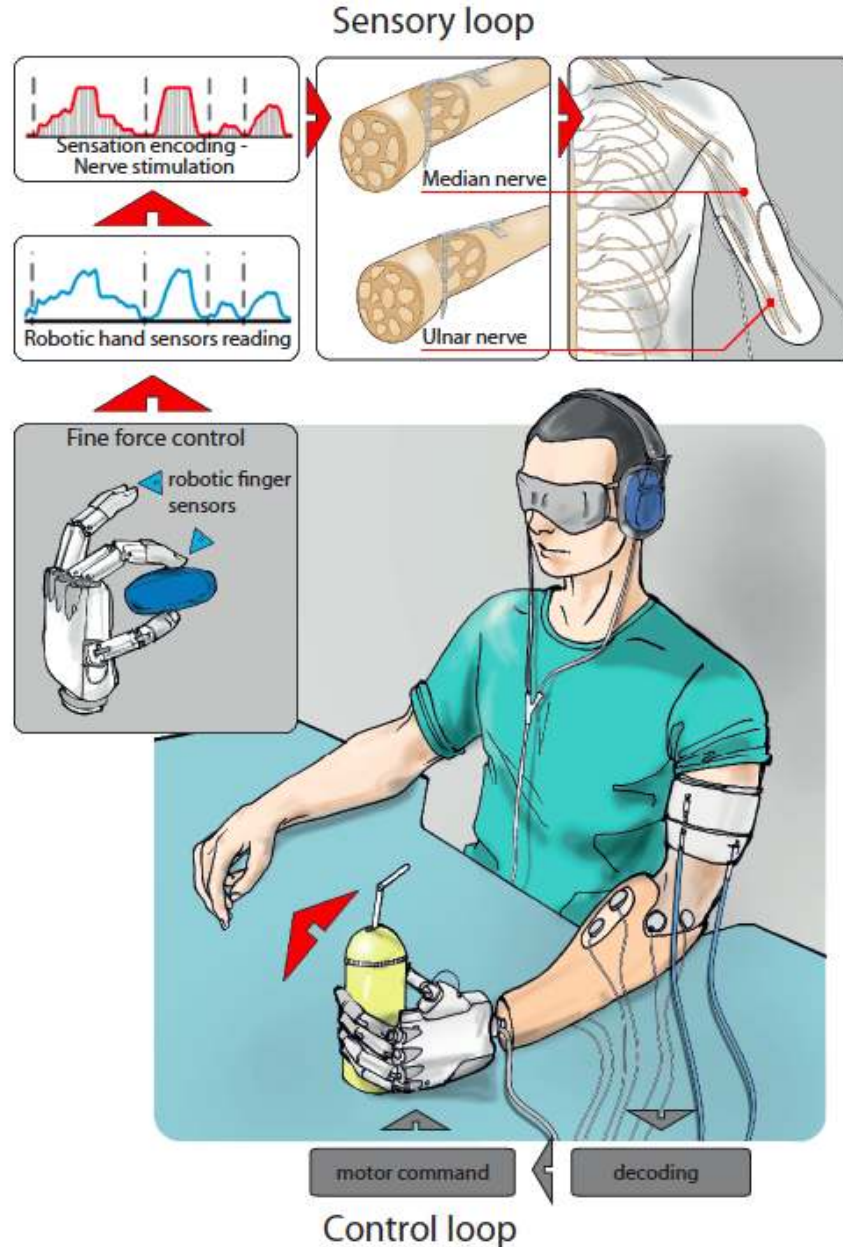


**Fig. 1 Bidirectional control of hand prosthesis.** During all the experiments the participant was blindfolded and acoustically shielded. The real time bidirectional control of hand prostheses involved both: (1) a reliable decoding of the user's motor command, immediately converted into hand motion (control loop in the figure) and (2) a simultaneous readout from prosthesis sensors fed back to the user, through intrafascicular nerve stimulation (encoding), in order to reproduce the innate touching sensations (sensory loop in the figure). The decoding was performed by processing sEMG signals, while encoding was simultaneously achieved by intrafascicular stimulation of the median and ulnar nerves, using TIME electrodes (25), with a delivered current profile consistent with the prosthetic hand sensors readouts.

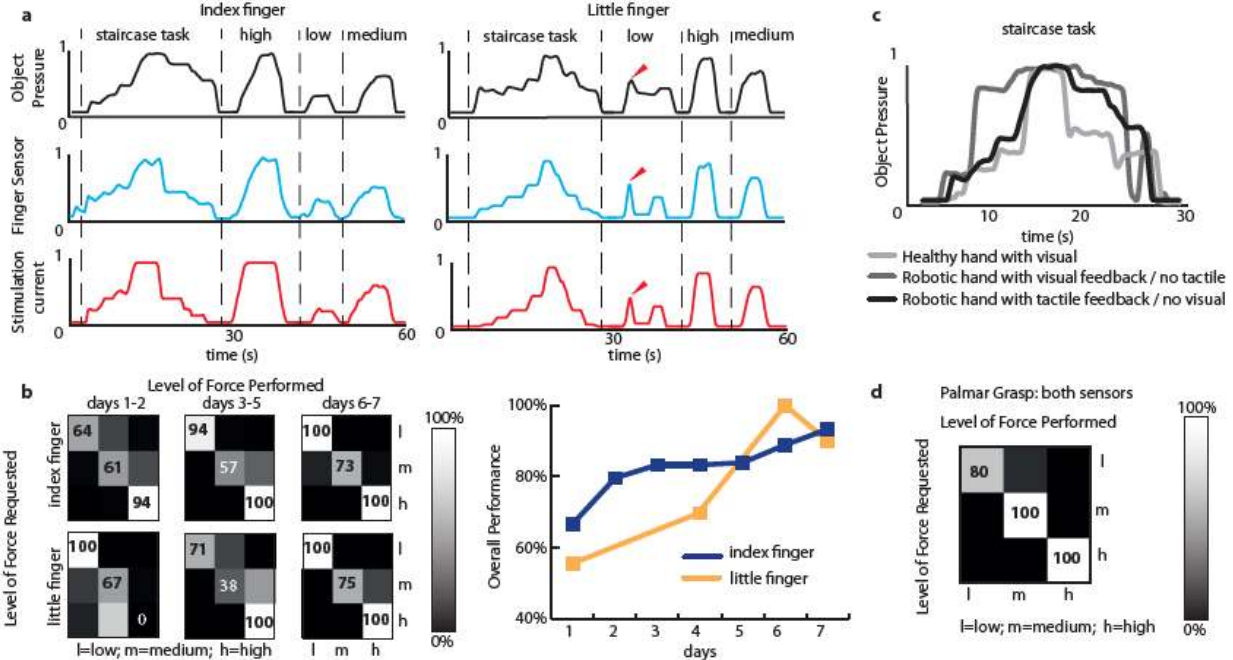


**Fig. 2 Fine force control.** The participant was asked to use the bidirectional robotic hand to produce one of three predetermined force levels over a pressure sensor, while performing pinch (panel **a**, index finger), ulnar (panel **a**, little finger) or palmar grasps (panel **d**). The participant was blindfolded and acoustically shielded and had to reproduce a "staircase task", in which he had to go gradually from a low to a maximum force level in 3 steps, then back to low in two subsequent steps. He then had to reproduce a randomly-generated sequence of pressure levels (**a**). In order to achieve the task, he had to use the sensory information provided by the electrical stimulation (red traces in **a**) which was computed using the finger sensor readouts (blue traces in **a**). A red arrow in (**a**, little finger) indicates a trial in which the participant recognized that he had overshoot the requested force level and corrected the error by regulating the grasp accordingly. (**b**) Confusion matrixes of the requested levels of force for the index and the little fingers at different days along with the overall performances showing a learning-related accuracy increase trend during the experiment (the accuracy of each class is reported on the main diagonal). (**c**) Performance of the hand without sensory feedback stimulation compared in the "staircase task" with those of the robotic hand with induced tactile feedback and those of the healthy hand; the robotic hand with induced tactile feedback reproduced a more similar force trace to the healthy hand ( $R^2=0.8$ ). (**d**), Confusion matrix assessing the task accuracy of the subject by executing the same task with a palmar grasp. In this task, the participant integrated both types of sensory information to achieve a mean class accuracy of 93.3%.

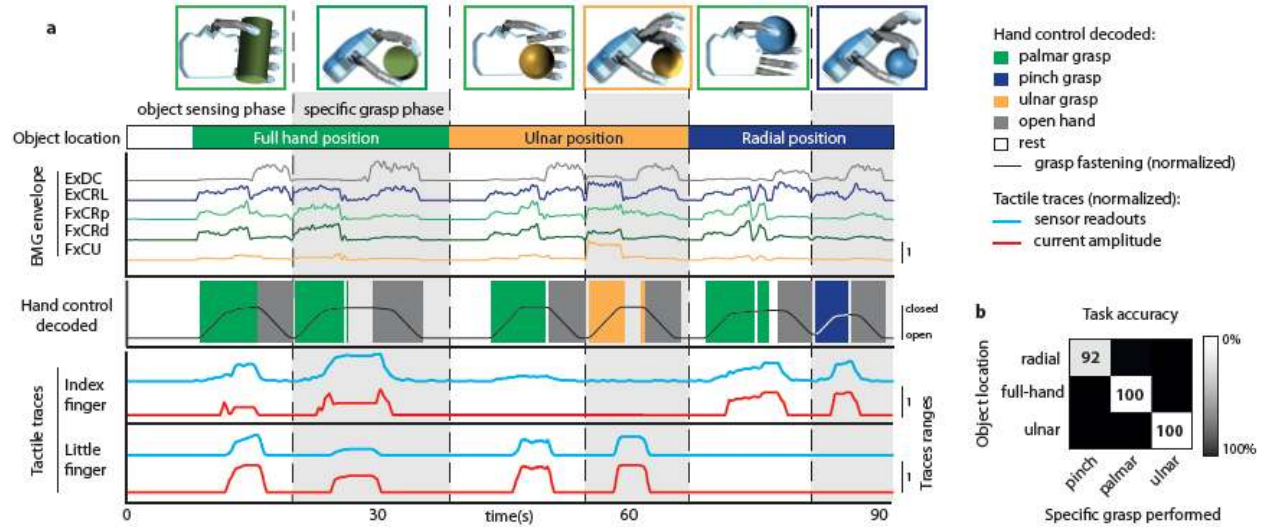


**Fig. 3 Object sensing and choice of the appropriate grasp for handling.** (a) Each of the three repetitions of the task involved a different location for the object (Object location). The participant first had to perform a palmar grasp to detect the object's position (sensing phase), then to release the grasp and perform the appropriate grasp for handling the item (specific grasp phase – shaded). The object was released once firmly grasped and then displaced with a translation movement by the arm. sEMG signals for extensor digitorum communis (ExDC), extensor carpi radialis longus (ExCRL), flexor carpi radialis proximal and distal (FxCRp, FxCRd) and flexor carpi ulnaris (FxCU) were recorded (EMG envelope) and processed to decode the user's hand control (decoded hand control), which drives the robotic hand opening/closure. The sensory feedback, encoded in terms of the intensity of intrafascicular nerve stimulation, arithmetically depends on the finger sensor traces (tactile traces). (b) Confusion matrix assessing task accuracy, based on the grasp choice following the object sensing phase, showing a mean class accuracy of 97.2% over 52 repetitions (the accuracy of each class is reported on the main diagonal).

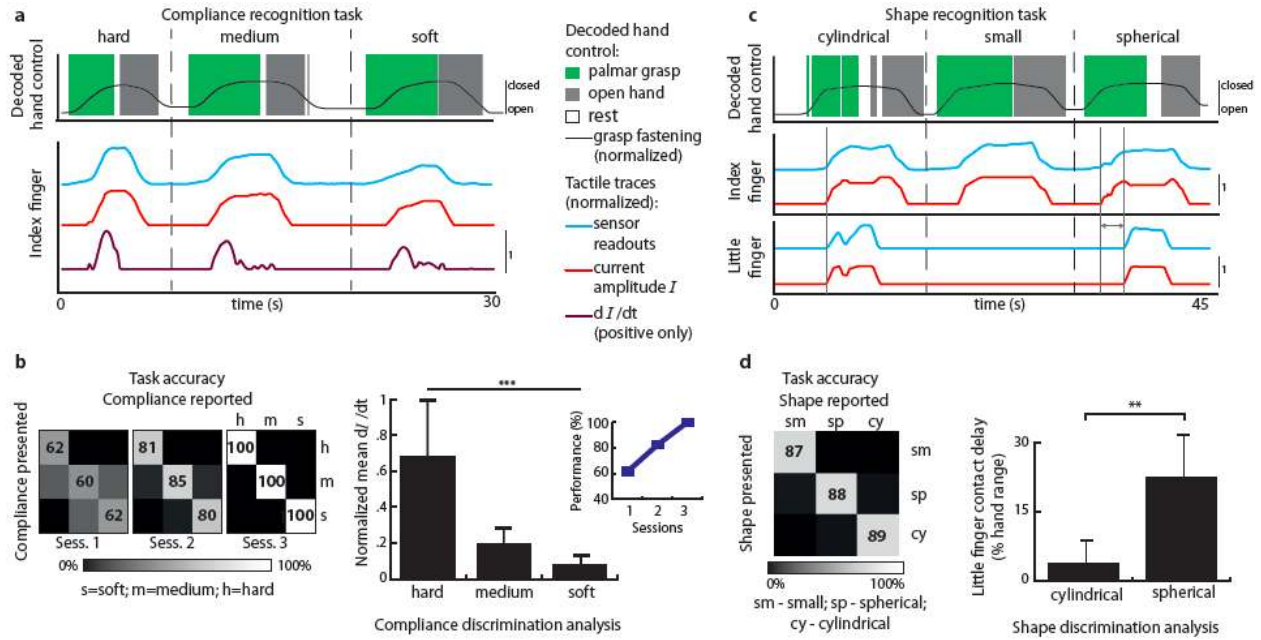


**Fig. 4 Object compliance and shape recognition.** (a) Each of the three repetitions of the task involved different object compliances, reported above the graphs. The participant performed a palmar grasp to explore the physical property of the object, then reported his sensation and released the grasp. Top: hand control decoded from sEMG activity. Bottom: index finger robotic hand sensor readout and corresponding intensity of nerve stimulation, with its positive time derivative. (b) Left: confusion matrixes assessing task accuracy, based on the sensed object's compliance reported by the subject, showing a mean class accuracy rising to 100% at the third session (right), over 14 repetitions. Center: the rate of growth of the tactile stimulation intensity applied during hand closure was significantly different between objects, thus providing a robust discriminating factor. (c) Each of the repetitions of the task involved a different shape, reported above in the graphs. The participant performed a palmar grasp to explore the physical property of the object, then reported his sensation and released the grasp. Top: hand control decoded from EMG activity. Bottom: index and little finger robotic hand sensor readout and corresponding amplitude of delivered peripheral nervous system (PNS) stimulation. The solid vertical lines and the grey double arrow indicate the stimulation onset delay between the radial and ulnar sites, if, during the manipulation, both parts of the hand get in contact with the object. (d) Left: confusion matrix assessing task accuracy, based on the shape of the sensed object reported by the subject, showing a mean class accuracy of 88% over 32 repetitions. Right: contact delay between the index and the little finger during manipulation was significantly different between objects that engage the full hand, thus providing a robust discriminating factor. \*\*,  $p < 0.01$ . \*\*\*,  $p < 0.001$ . Error bars, s.d.

## **Supplementary Materials**

### **Materials and Methods**

#### ***Subject and experiments***

The subject DAS had suffered a transradial left arm amputation 10 years ago, as a consequence of a traumatic event. He was selected from a group of 31 people with hand amputation because of the characteristics of the stump and his psychophysical abilities. He was surgically implanted with intrafascicular electrodes and, by means of voluntary contractions of the stump muscles, he controlled several degrees of freedom of a prosthetic hand. During all experiments, the participant was blindfolded and acoustically shielded in order to eliminate both visual and auditory feedback. He did not receive any particular training, and quickly learnt how to use the bidirectional control of the robotic hand.

During the controlled pressure task (fine force control), the subject was instructed to produce three different force levels using the bidirectional robotic hand, and to hold them for at least 2 sec. Depending on the experiment, he was engaged either in repeated up-down transitions from lowest to highest sensed pressure levels (staircase task) or single-level press-and-release trials, where he was asked to randomly replicate the generated sequence of pressure levels. The experiments were repeated for pinch, ulnar, or palmar grasps, each produced over a pressure sensor chamber.

In the functional exploration tasks (object sensing and choice of the appropriate grasp for handling), the subject controlled a voluntary palmar grasp in order to understand, through sensory feedback, the location (ulnar, radial or full hand) over his hand of an object and then to grasp it with an appropriate command and deliver it to the experimenters (in both the radial and ulnar locations, but with different arm motion directions) or raise it (bottle).

During the object compliance recognition task he was asked to grasp objects with different compliances and to rely on the sensory feedback to understand the specific physical property. Finally, in the object shape-recognition task, the subject had to perform a palmar grasp to explore the object topology of three possible shapes, then report his sensation and release the grasp.

All procedures were approved by the Institutional Ethics Committees of Policlinic A. Gemelli at Catholic University, where the surgery was performed, IRCCS S. Raffaele Pisana (Rome), where the experiments were performed, the Ethics Committee of Campus Bio-Medico University and the Italian Ministry of Health.

#### ***Surgical procedure***

In general anesthesia, through a 15 cm-long skin incision on the left arm, the median and ulnar nerves were exposed to implant a proximal and a distal TIME electrode in each one. The microelectrodes and a segment of their cables were brought into the operating area across four small skin incisions, two laterally and two medially to the main surgical cut. The cable segments were placed in subcutaneous pockets and secured with sutures. Then, using an operating microscope (Zeiss, Pentero), the single microelectrode was implanted transversally within the nerve fascicles; appropriate microsutures secured the nerve implant. This implantation procedure lasted seven hours requiring a number of careful procedures necessary to guarantee the stability



of well-functioning microelectrodes (including impedance measurements of individual contacts) not only for the duration of the experiment but permanently.

After 30 days, under an operating microscope the four microelectrodes were removed, in accordance with EU guidelines. At the time of removal however, the TIME electrodes were still performing extremely well, and did not cause any discomfort to the subject. The follow-up of the clinical condition of the participant 2 months after the end of the protocol did not reveal any subjective or objective side-effects.

### ***Real-time bidirectional control***

#### *Transformation of EMG signals into the robotic hand commands (decoding)*

The sEMG signals were collected differentially (surface disk electrodes in a belly-tendon montage) at five sites on the stump, corresponding to the three muscle bellies of Flexor Carpi Ulnaris (FCU), Extensor Carpi Radialis Longus (ECRL) and Extensor Digitorum Communis (EDC) and two additional recording sites located on a proximal and distal position of Flexor Carpi Radialis (FCRp and FCRd), with a grounding site at the Olecranon to complete the setup. Data were sampled at 12 kHz, analogically band-pass filtered between 100 and 1000 Hz, and amplified  $\times 10000$ , by means of the commercial amplifier, QP511 from GRASS. They were then collected at intervals of 100ms, so as to generate the classification feature vector. These 1200 samples per channel were then divided in two bins of 50ms. The following parameters were extracted for each of these sequences:

- Signal Variance (29, 30);
- First half of the FFT components integrated (30);
- Second half of the FFT components integrated (30);
- Difference between the amplitude of the first and the second half of the bin samples (30).

All the features extracted were stacked and processed by a 3-layer multi-layer Perceptron (MLP) network that provided one output node for each possible hand motion, plus an additional one for the rest state. The decoded state competition at the final layer was solved by a winner-takes-all strategy. The MLP was trained using a supervised learning approach after a set of EMG data had been collected in a specific initial session of approximately 50 seconds, in which the subject was asked to imagine performing a sequence of three 2s-long repetitions for each hand movement that had to be classified by the network ('Pinch Grasp', 'Little Finger Grasp', 'Palmar Grasp', 'Hand Opening'), separated by two-second rests. During on-line classification, possible chatter from the MLP output was smoothed using hidden Markov model (HMM) filtering; i.e. the current state of the user's desired hand control  $x(t)$ , which was assumed to have generated the last observed instance of the EMG signal feature vector  $y(t)$ , was estimated by choosing the most likely value of the distribution  $P(x(t)|y(1), \dots, y(t))$ . The HMM transition weights were fixed at 0.5 to keep the current state, and at 0.1 to switch to any new state.

The final output was transferred to the robotic hand within a soft real-time deadline set at 100ms, when the next sEMG signal block was made available. The desired hand motion was driven in terms of position control, resulting in a progressive opening or closing of the fingers involved in the user-selected grasp by approximately 2% of their motion range per output evaluation cycle when the finger sensors did not report contact with an object, and 0.5% in the other cases.

#### *Transformation of sensors readouts in stimulation patterns (encoding)*

The sensors embedded in the hand prosthesis were used as inputs for the delivery of the afferent neural stimulation. A commercial stimulator from Multichannel System (8 channel, STG4008 16 mA) was used during the experiments.

The relationship between the hand sensors and the amplitude of the stimulation current biphasic pulses delivered was implemented as follows:

$$c = \begin{cases} \left( \frac{s - s_{15}}{s_{75} - s_{15}} \right) * (c_{max} - c_{min}) + c_{min}, & s_{15} \leq s \leq s_{75} \\ 0, & s < s_{15} \\ c_{max}, & s > s_{75} \end{cases},$$

where:

$c$  is the amplitude of stimulation current,

$s$  is the readout sensor,

$s_{15}$  and  $s_{75}$  represent 15% and 75% respectively of the maximum range of the sensor readout, which characterize the contact point of the robotic hand with an object and a value tuned to exploit the full range of sensations for all objects, respectively,

$c_{min}$  and  $c_{max}$  are the stimulations that elicited the minimum and the maximum (before feeling pain) sensations for the subject, respectively.

The stimulation, which was sent continuously to the subject, was updated every 100 ms. Specifically, the soft real time algorithm dedicated to the sensory loop was able to read both hand sensors' outputs and to encode the respective sensory stimulation within this time frame of 100 ms. Simultaneously, the algorithm dedicated to the control loop was able to acquire, process, decode the sEMG signals and to deliver the motion command to the robotic hand, all within the same 100 ms frame, which is imperceptible for a prosthesis user (24).

### *Analysis of data*

Statistical evaluations were performed for the functional exploration and the compliance recognition tasks. All data were reported as mean values  $\pm$  standard deviations. The Kruskal-Wallis test was performed when the data sets were not normally distributed. The Tukey-Kramer test was applied in the case of three groups of data.



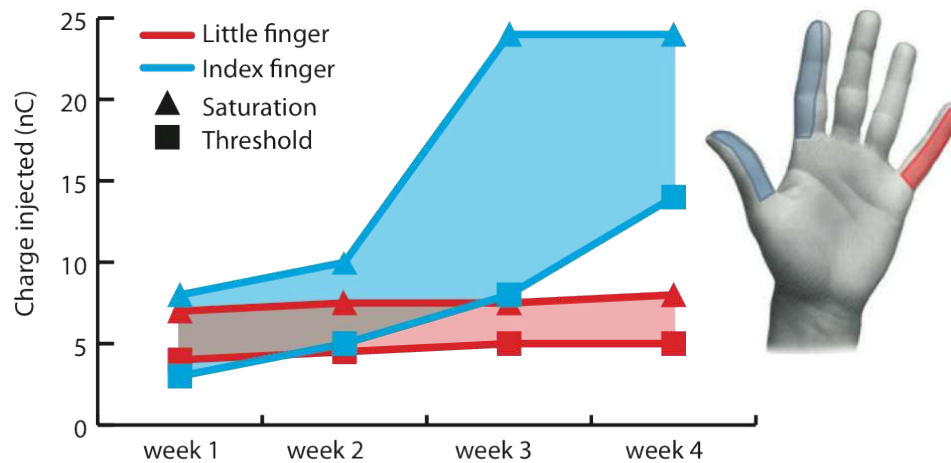


**Fig. S1 - Stimulation properties of neural electrodes.** Sensation threshold corresponded to the minimal pressure reported, while saturation (or “pain-threshold”) was defined as the charge that elicited nearly painful pressure. The sensation positioning was remarkably stable and repeatable. Reported values of injected charge are in nanocoulomb (nC). Stimulation of the ulnar nerve produced the sensation of gradual touch in the little finger (red). In addition, the values for both threshold and saturation were also very stable. Stimulation of median nerve produced the sensation of gradual touch in both index finger and thumb. The range and feeling for its stimulation remained stable, though it changed, in absolute values, slightly over 3 weeks. Both values were much lower compared to the maximum charge injectable by means of TIME devices (120 nC).

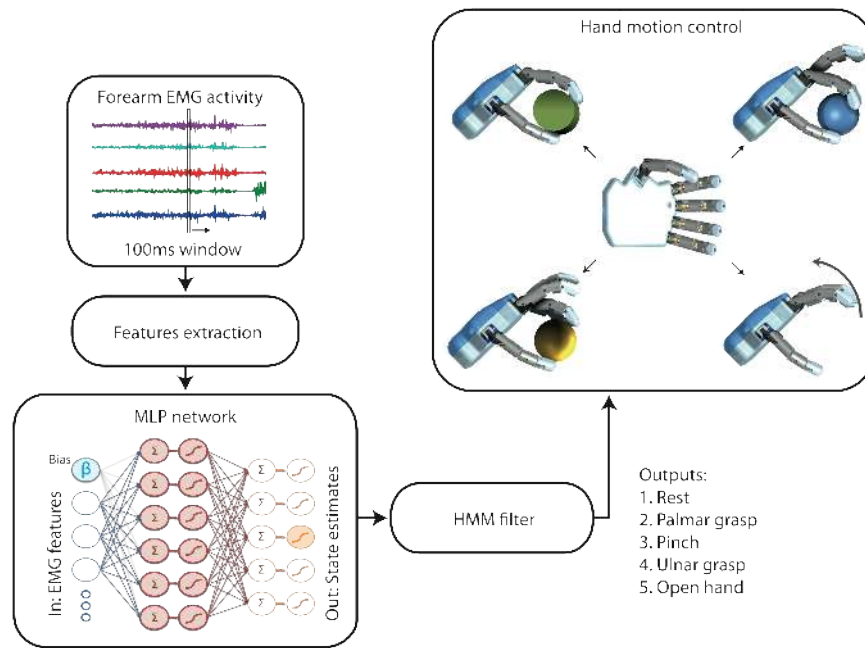


**Fig. S2 - Processing of surface electromyographic (sEMG) signals to control the hand prosthesis.** sEMG signals were collected at five sites on the residual forearm, at intervals of 100 ms to generate the classification feature vector. Signal variance, high and low terms of the FFT and the difference between the amplitude of the first and the second half of the bin samples were computed and used as classification features. These signals were processed by a Multi-Layer Perceptron (MLP) network that provided one output node for each possible hand motion, plus an additional one for the rest state. During on-line classification, possible chatter from the MLP output was smoothed using hidden Markov model (HMM) filtering. The resulting decoded state was used to control the hand motion.

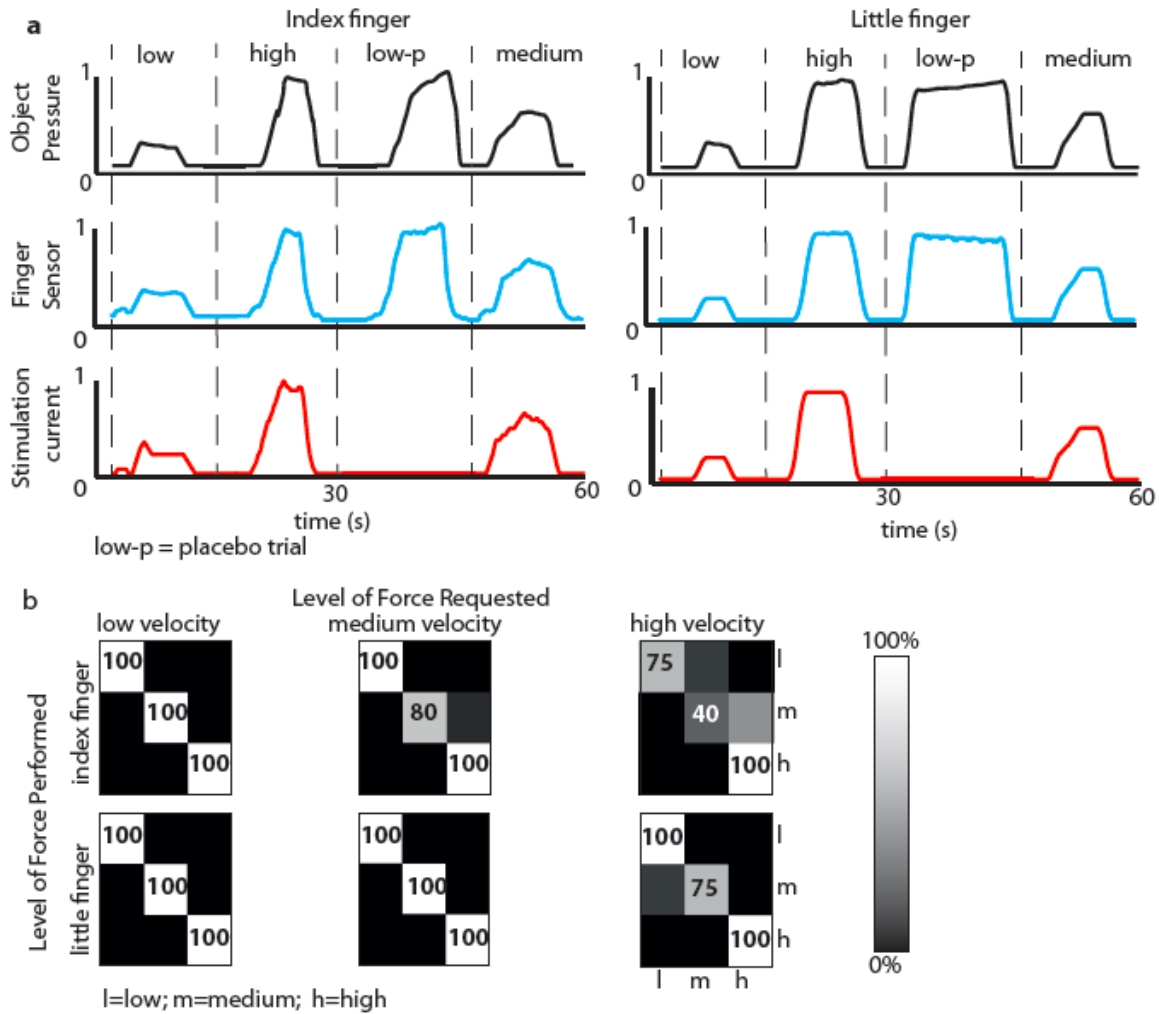


**Fig. S3 - Fine bidirectional control is entirely due to the integration of the restored sensation into the bidirectional loop.** Examples of placebo trials, randomly mixed during the sessions of the fine force protocol are showed in panel (a), *low-p*. The participant was blindfolded and acoustically shielded and was asked to perform the minimum level of force but with the electrical stimulation turned off (no feedback from the sensors of the hand prosthesis). Without any tactile information, the subject was not able to achieve any kind of control eliciting a very high level of force before releasing the object, which he was not able to sense. The performances at different velocities of the hand motors were tested (b). As expected, when the motor velocity was set to the lowest value, the participant produced his best performances, while at higher velocities he performed the worst. This is expected for a bidirectional prosthesis in which information regarding the elicited force relies only on induced tactile information. At higher velocities the subject found it more difficult to finely control the movements, while at lower velocities he was able to finely grade the force. If the participant relied on the time needed for the hand to close, to control the elicited force, then he would also have performed badly at lower velocities, whereas he actually performed much better, thus proving that the force control only relied on the sensory tactile feedback.

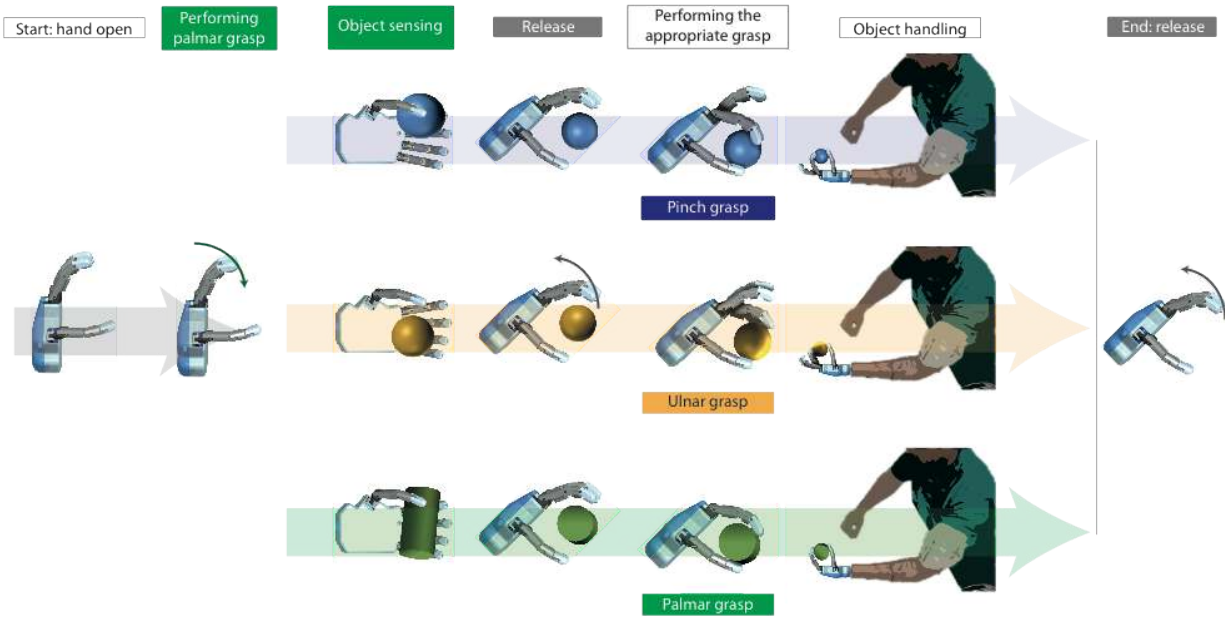


**Fig. S4 - State flow chart for the manipulation task (object positioning sensing and handling task).** The participant, blindfolded and acoustically shielded, is performing a palmar grasp to sense the location of the object that might be in a radial, ulnar or full hand position. Once he has recognized this spatial information, he releases the object and performs a location-specific grasp to handle the object: pinch for the radial location, ulnar grasp for the ulnar location and palmar grasp in the full-hand case. When the object is grasped firmly, the participant is required to displace it with a full-arm movement and to release the grasp.

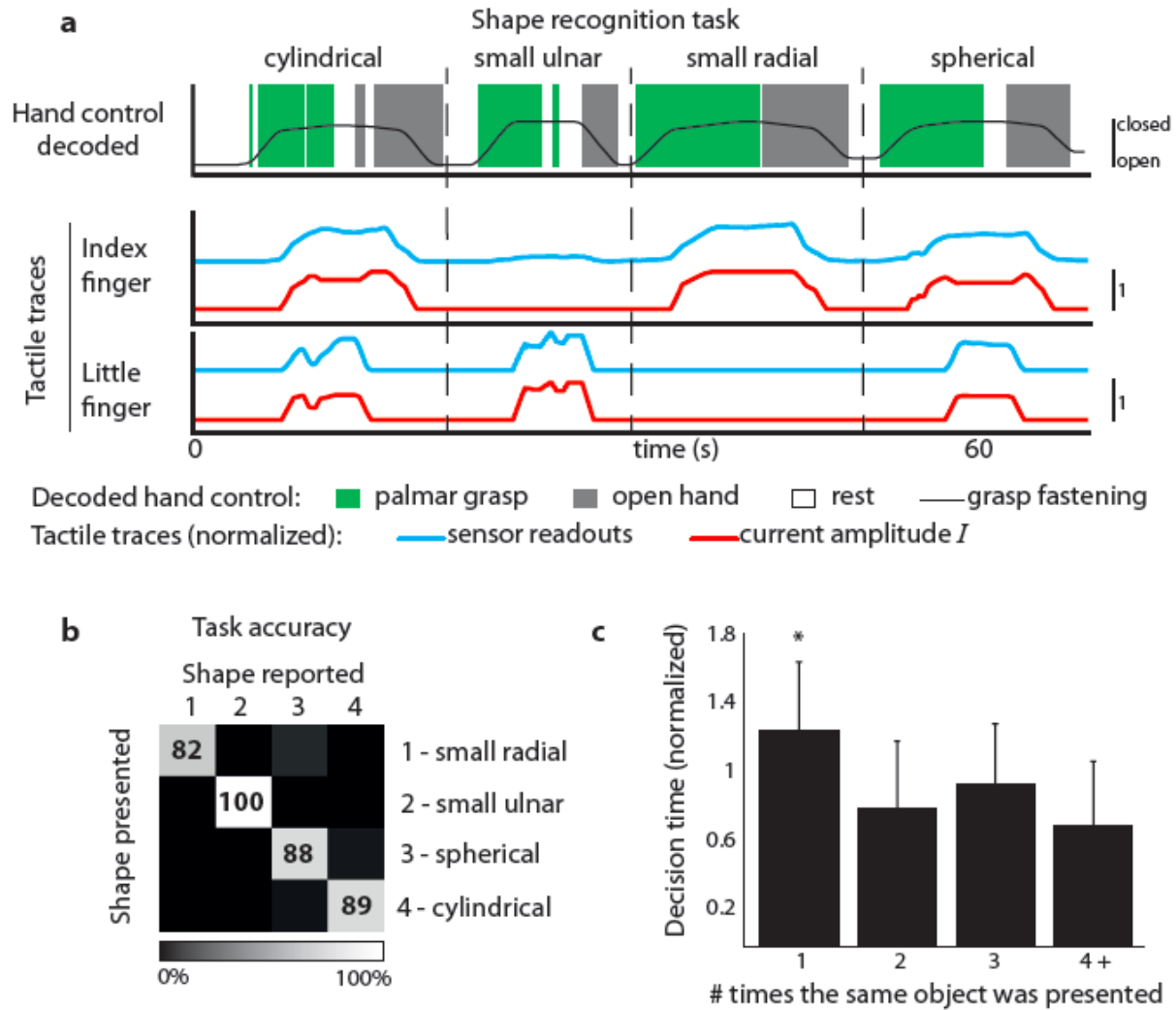


**Fig. S5 - Shape recognition separated by location of the small object and time necessary for correct classification. (a)** Each of the task repetitions involves the same object shapes reported in Figure 4, but separates the small object trials into two categories for ulnar or radial nerves. The participant performed a palmar grasp to explore the object shape and then reported his sensation while releasing the grasp. Top: hand control decoded from sEMG activity. Bottom: index and little finger robotic hand sensor readout and corresponding amplitude of delivered PNS stimulation. **(b)** Confusion matrix assessing the task accuracy, based on the sensed object's shape (and ulnar or radial location in the case of the small object) reported by the subject, showing a mean class accuracy of 89.8% out of 32 repetitions. **(c)** The time needed for the participant to discriminate between objects decreased as the same object was repeatedly presented. Decision time is measured in the time delay between finger contact with the object and the first decoded occurrence of the decision to release the grasp, normalized to unitary mean by session and object. The time taken to achieve the discrimination the first time an object was presented during a session is significantly higher than the time taken in each of the subsequent times the same object was presented. \*,  $p < 0.05$ . Error bars-s.d.

**Movie S1: Functional exploration and object handling.** After the start cue, the participant - blindfolded and acoustically-shielded - made a palmar grasp over the object. Objects were placed at three different positions close to the robotic hand: ulnar, radial and full hand. As soon as he has understood and verbally indicated the object position, the participant open the hand, performs an appropriate grasp and manipulates the object. He had to deliver the object to the experimenter in front of him (in case of radial position), to the experimenter on his right (in the case of ulnar position) and lift it up (in the case of full-hand sensing). A close-up of the hand manipulation during the 'sensing phase' is provided in the latter part of the movie.

**Movie S2: Recognition of object compliance.** The experimenter presented to the participant, blindfolded and acoustically shielded, three objects with different compliances (hard, medium, and soft), placing them in radial position. The participant, after a triggering signal given by the experimenter, grasped the object and sensed its compliance by relying only on the sensory feedback.

## References

29. K. Englehart and B. Hudgins, A robust, real-time control scheme for multifunction myoelectric control. *IEEE Trans. Biomed. Eng.* 50, 848–854 (2003).

30. M. Zecca, S. Micera, M. Carrozza, and P. Dario, Control of multifunctional prosthetic hands by processing the electromyographic signal. *Crit. Rev. Biomed. Eng.* 30, 459–85 (2002).

## Any Additional Author notes

### *Author contributions*

*S. Raspopovic: designed the study, developed the software, performed the experiments and wrote the paper.*

*M. Capogrosso, M. Bonizzato and F. Petrini: developed the software and the overall system integration, performed the experiments, analyzed the data and wrote the paper.*

*J. Rigosa: developed the software and collaborated during the experiments*

*G. Di Pino: selected the patient, collaborated during the design of the study and during the experiments.*

*J. Carpaneto, G. Granata, L. Citi, A.L. Ciano, C. Oddo: collaborated to the integration of all the components of the device, collaborated during the experiments.*

*M. Controzzi, C. Cipriani and C. Carrozza: developed the robotic hand.*

*W. Jensen, E. Guglielmelli: collaborated to the preparation and execution of the experiments.*

*T. Boretius and T. Stieglitz: developed the TIME electrodes.*

*E. Fernandez: performed the surgery.*

*PM. Rossini: selected the patient, designed the study, and wrote the paper.*

*S. Micera: designed the study, supervised the experiments, and wrote the paper.*